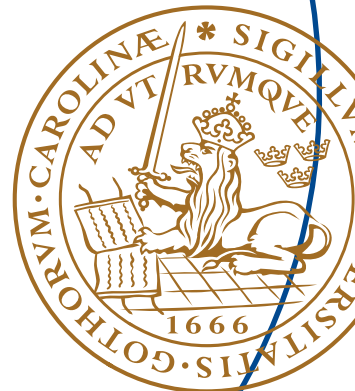


Master's Thesis

**Performance Evaluation of
Distributed Antenna Systems:
Comparison using the
COST 2100 Model and
Measured Channels**

Panagiotis Papaioannou



Performance Evaluation of Distributed Antenna
Systems: Comparison using the COST 2100
Model and Measured Channels

Panagiotis Papaioannou
wir12ppa@student.lu.se

Department of Electrical and Information Technology
Lund University

Advisor: Ghassan Dahman

May 22, 2016

Abstract

Modern wireless technologies strive to meet users’ ever increasing demand for high data rates and improved services. One of the most important constraints in wireless system performance is interference. More specifically, the interference caused by serving multiple users in the same geographical area can degrade the link quality greatly.

A possible solution to the aforementioned problem is to utilize Coordinated Multi Point (CoMP) transmission and reception techniques. A system that operates using CoMP is capable of dynamically coordinating its transmission and/or reception in order to achieve improved performance. CoMP technology is already adopted by 3GPP for the LTE-Advanced system and numerous studies took place in order to investigate deployment scenarios on that platform. In this work the performance evaluation of different CoMP transmission techniques will be presented. The performance evaluation will be performed using two approaches. In the first approach, the performance evaluation will be based on channel matrices collected from a measurement campaign at Lund University. In the second approach, the different realizations of the channel matrices are generated using the COST 2100 channel model. Then, the results of the two approaches are compared.

It was found that, performance evaluation using the COST 2100 can describe the relative performance of the studied CoMP transmission techniques compared to the measurements.

Table of Contents

1	Introduction	1
1.1	CoMP transmission schemes	1
1.2	Coordination and channel estimation	3
1.3	Background	4
1.4	Thesis scope	5
2	System Model	7
2.1	Coordinated beamforming	7
2.2	Joint Processing (JP)	8
2.3	Partial Joint Processing (PJP)	8
2.4	Sum rate capacity	9
2.5	Transmit beamforming vectors	10
3	Channel Matrix Generation and the COST 2100 model	13
3.1	Visibility Region (VR)	14
3.2	COST 2100 features	14
3.3	COST 2100 Implementation	15
4	Propagation Measurements	17
5	Results	21
5.1	Performance evaluation under measured channel matrices	21
5.2	Performance evaluation based on generated channel matrices using COST 2100	25
5.3	Performance Comparison between measured channel and COST 2100 channel	26
5.4	System performance variation based on inter-user distance	29
5.5	Changing the COST 2100 model parameters	31
6	Conclusions	39
7	Future work	41
	References	43

List of Figures

1.1	Instances of a CoMP system	2
2.1	System representation of the coordinated beamforming scheme.	7
2.2	A JP scheme with 3 BSs communicate with MS 2.	8
2.3	A PJP scheme with MS_2 having 2 BSs in its active set.	9
2.4	Illustration of the leakage term in a multi-user system.	10
3.1	COST 2100 channel structure [1].	14
3.2	Illustration of the VR under the COST 2100 channel model [1].	14
4.1	The RUSK LUND channel sounder used in the measurement campaign.	17
4.2	The path under which the measurement campaign took place. The simulated users were placed along this trail.	18
4.3	Photo of a part of the measurement route showing the MS unit.	19
5.1	Sum rate capacity for 6 randomly distributed users when SNR =15dB is considered. The results are based on the channel matrix generated by the measurement data.	22
5.2	Sum rate capacity for 4 and 8 randomly distributed users when SNR = 15dB is considered. The results are based on the channel matrix generated by the measurement data.	22
5.3	Sum rate capacity for different number of uniformly distributed users with 5m spacing on the left and 10m spacing on the right.The channel matrix was generated from the measurement data.	24
5.4	Sum rate capacity for 6 randomly distributed users when SNR =15dB is considered. The channel matrix was generated using the COST 2100 model.	25
5.5	Sum rate capacity for 4 and 8 randomly distributed users for SNR =15dB. The channel matrix was generated using the COST 2100 model.	26
5.6	Sum rate capacity for different number of uniformly distributed users with 5m spacing on the left column and 10m spacing on the right column.The channel matrix was generated using the COST 2100 model.	27

5.7	Comparison of CoMP techniques between the COST 2100 and measured channel. These results assume 6 randomly distributed users and SNR = 15dB.	28
5.8	Performance comparison of CoMP transmission schemes under the COST 2100 and measured channels. The graphs shown here correspond to 6 users with 10m separation and SNR =15dB.	30
5.9	Sum-rate capacity variation with respect to inter-user distance change. The base case is 5m. The 3 rows correspond to 4,6 and 8 users in the system respectively.	32
5.10	PJP performance for COST 2100 channels generated based on Table 5.4. The results assume 6 randomly distributed users and SNR = 15dB.	34
5.11	PJP performance for COST 2100 channels generated based on Table 5.5. The results assume 6 randomly distributed users and SNR = 15dB.	35
5.12	Sum-rate capacity of the PJP scheme for different distributions of the VRs. The results assume 6 randomly distributed users and SNR = 15dB.	36
5.13	Illustration of the VRs locations. The VRs are shown with white, the BSs locations are marked with yellow and the possible user locations with blue.	37

List of Tables

5.1	Concentrated results for the sum-rate capacity performance between the COST 2100 generated channel and the measured one. The results presented in the table assume SNR =15dB and random user distribution.	29
5.2	CoMP transmission schemes sum-rate performance for uniformly distributed users in the simulation area for SNR =15dB. The results consider the 50th percentile of the capacity curve.	31
5.3	Initial COST 2100 channel parameters. The simulations up until this point used these values.	32
5.4	LOS VR size for different variations of the COST 2100 channel model.	33
5.5	The values for the VR size of different generated COST 2100 channels.	34

Introduction

Coordinated Multi-Point (CoMP) is a technology that emerged in order to deal with the inter-cell interference (ICI) caused by using the same resources in neighboring cells. The cell-edge users are affected the most from ICI, reducing the average cell throughput and degrading the performance of the system. CoMP schemes can also be used to improve the performance of a single cell by utilizing multiple transmission points to communicate with a single user. CoMP schemes can be used for both transmission and reception and the antenna elements used in the system are geographically distributed and coordinated. Both the transmission and reception CoMP schemes can be used to improve the performance of the cell. The CoMP entities are depicted in Fig.1.1 and are the:

- Remote radio unit (RRU)
- Cells, that implement intra-BS or inter-BS coordination
- Relay Nodes (RNs)

There are two CoMP transmission schemes namely Joint Processing (JP) and Coordinated Scheduling and/or Beamforming (CS/CB). The entities that participate in the CoMP scheme comprise a CoMP cooperative set [2]. The elements of the cooperative set receive scheduling information from a central unit so that the average cell and cell-edge throughput is improved. The central unit schedules the BSs that will participate in the cooperative set based on the channel quality information that receives from each BS in the vicinity.

1.1 CoMP transmission schemes

This section will familiarize the reader with the coordinated techniques mentioned above.

1.1.1 Joint Processing

In JP, user data is available to all the BSs belonging in the cooperative set. A further classification of the JP scheme can be done into two categories, Joint transmission (JT) and Dynamic Cell Selection (DCS). In this study only the JT

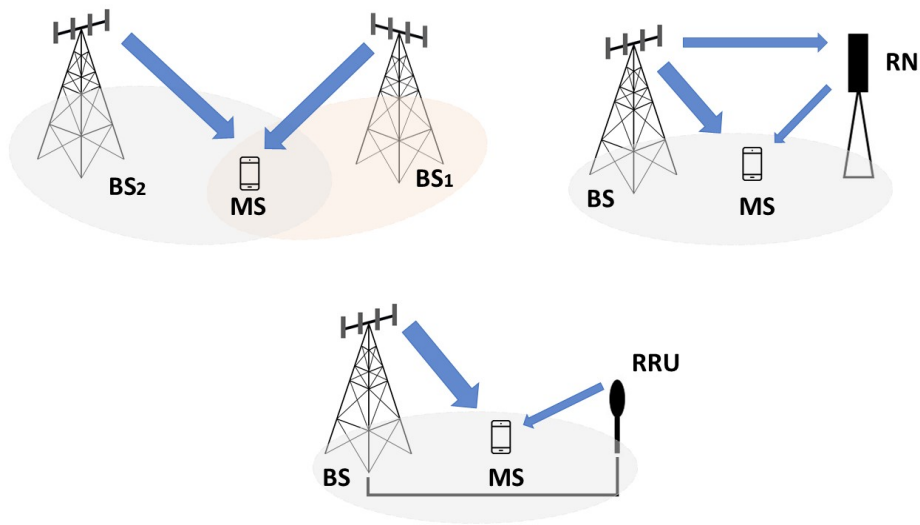


Figure 1.1: Instances of a CoMP system

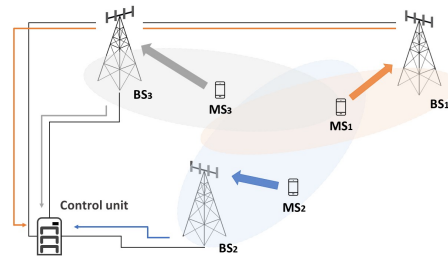
will be consider and from this point forward referring to JP will imply the use of the JT.

In JP the same user data is transmitted to a specific User Equipment (UE) from all the BSs of the cooperative set thus improving the received signal quality. The coordination of the BSs is organized by a Central Unit (CU) that decides on the power levels and the beamforming weights. Tight synchronization between the entities of the cooperative set must be available, which can be considered as a drawback, although with the cost of optic-fibers being significantly lower nowadays that task is considered plausible.

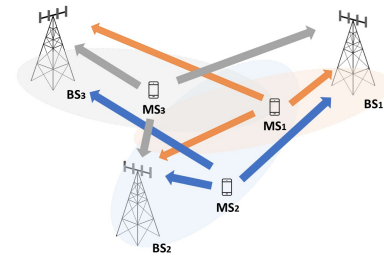
Partial Joint Processing

The disadvantage with JP is that the information for the UE must be available to all the BSs belonging to the cooperative set thus the backhaul requirements are high [3].

The Partial Joint Processing (PJP) is a special case of JP and is able to reduce the information exchange between the cooperative BSs and the user feedback to the network. In PJP not all the BSs transmit user information unless they belong to the active set of the user. The active set changes its cardinality based on the channel gain of each BS. More specifically, each user is assigned a master BS which is the one with the highest channel gain. The remaining BSs in the cooperative set are added in the active set only if their channel gains are higher than a threshold with respect to the master BS. The value of the threshold is specified by the CU and choosing a low value will lead to a full JP scheme.



(a) Centralized CoMP architecture



(b) Decentralized CoMP architecture

1.1.2 Coordinated Beamforming

In Coordinated Beamforming (CB) only a single transmission point is considered while the rest of the points in the cooperating set are coordinated to take beamforming and scheduling decisions. This method is used for mitigating the interference coming from transmissions intended for other UEs of the same or neighboring cells. As a result the interference is reduced to the cost of committing more than one antenna elements per UE [4]. On the contrary, the user data do not need to be available in all the BSs like in JP which reduces the load on the backhaul.

1.2 Coordination and channel estimation

There are two different CoMP architectures depending on the way the Channel State Information (CSI) becomes available to the cooperative set, centralized and decentralized coordination [3]. These approaches can be applied to both JP and CB although here only the coordination for a JP scheme is described. In this work the centralized coordination approach is considered.

1.2.1 Centralized coordination

Assuming an Frequency Division Duplex (FDD) system is used, the following procedure occurs to exchange information between the cooperative set. The UEs need to estimate the CSI related to all the BSs in the set and report their estimate back to the network. The CU gathers the Channel Quality Indicators (CQIs) from all the UEs and performs user scheduling and the precoding design. Since this is a JP scheme user data must be available at all the BSs in the cooperative set. This necessitates the BSs to be time-synchronized.

In the case of Time Division Duplex (TDD) systems the downlink CSI can be obtained from the uplink using the principle of channel reciprocity. Thus the overhead is reduced since the UEs do not need to return the CSI back to the BSs. The BSs involved must again send their estimate back to the CU.

1.2.2 Decentralized coordination

In order to decrease the overhead and the communication between the CU and the BSs the decentralized approach can be used. A method like the one described

in [5]. In this solution the UEs estimate the CSI related to all the cooperating BSs and then feed back the estimates to all the cooperative BSs. Hence, each BS acquires channel information locally and remotely. This architecture provides the benefit of minimizing the communication between the CU and the BSs by reducing the backhaul strain and signaling cost. Consequently, already deployed systems do not need great changes to accommodate a CoMP scheme [6]. Furthermore, the radio feedback to several nodes could be achieved without additional overhead. On the contrary, studies have shown that this technique is prone to errors on the uplink [7] since the wireless links between the UE and the different BSs can vary greatly. Thus ways to mitigate this issue must be found like the one presented in [8].

Another approach to consider, is the use of mixed implementations of these architectures as they will combine the advantages of the aforementioned schemes.

1.3 Background

Many studies have focused on the implementation impact of the CoMP techniques in terms of the capacity improvement like in [9] where 2 cooperative transmission techniques were used. The SINR improvement was substantial compared to conventional transmission methods and consequently the capacity was improved as well. The comparison in that study was done using a Gaussian channel and hence does not represent a realistic case. Moreover, only 2 CoMP were considered. The authors in [10] investigated the capacity discrepancies between a distributed MIMO system and a conventional MIMO system. The distributed MIMO as the authors refer to it, is a Distributed Antenna System (DAS) with MIMO elements. The DAS proposed there uses joint transmission to transfer the data to the UE and the results showed significant improvement in the capacity of the cell compared to the conventional MIMO. Despite using measurements in order to derive their conclusions, the authors only used the JP CoMP technique and their measurements took place in a urban environment. In [11] the authors showed that using CoMP will not only improve the throughput of the system but it will also reduce the transmission power. Their work is different from the one presented here as they used a simple Gaussian channel for their calculations and only the JP scheme to derive conclusions. The authors in [12] investigated the effects of CoMP in a macrocell environment through measurements. The authors took measurements in a urban environment and used JP as a transmission scheme. Comparatively to work presented here the measurements used took place in a sub-urban environment with the MSs having 1 antenna element. Also, the COST 2100 channel model was used to compare the results from the measurements. Other approaches to improve the throughput and/or the SINR were used like scheduling algorithms [13], varying the size of the cooperative set [14] or using power allocation algorithms [15]. The authors [13] used the JP transmission scheme and a flat Rayleigh fading channel compared to the presented approach were a realistic channel environment was created using the COST 2100 model. The work in [14] did not include a realistic channel representation as in considered only a pathloss model. The DCS scheme was used in [16] to demonstrate the SINR increase on the cell-edge users.

There was no comparison between the different CoMP transmission techniques though, and the channel used was Gaussian. In [17] different JP techniques were compared in terms of the achievable capacity. This work considered a realistic channel matrix generated from the WINNER II model but it did not touch upon the performance comparison between the different CoMP transmission schemes. Moreover, no measurements were used to compare the findings against the real environment. In [18] the authors explored the performance difference between a non-CoMP scheme against the JP and CB CoMP schemes. They used the 3GPP Spatial Channel Model (SCM) which considers MIMO systems but the number of antennas at the MS are 2 instead of 1 as used in this work. In addition, no measurements were used to verify their theoretical results. The authors in [19] presented the benefits of using the CB CoMP transmission scheme together with a feedback technique. No comparison between the Transmission CoMP techniques took place and the channel model that they used (e.g. 3GPP SCME) although realistic, is not as complete as the COST 2100.

1.4 Thesis scope

Despite the extensive research and to the author’s best knowledge there is not enough information regarding the comparison between all available CoMP techniques, namely: JP, PJP and CB. Also the majority of the studies presented above, use simulations to derive their results or unrealistic channel models.

In this thesis the Joint Processing (JP), Partial Joint Processing (PJP) and the Coordinated Beamforming (CB) CoMP transmission techniques will be evaluated in a microcell environment. Initially the CoMP transmission schemes will be evaluated under the COST 2100 channel model. Following, the same evaluation will take place using a channel matrix derived from measurements campaigns that took place in Lund University [20]. The users will be placed in the simulation area following two different distributions, random and uniform, for the purpose of evaluating the impact on the system’s performance with respect to the inter-user spacing. In the final stage of this work a more detailed comparison between the COST 2100 and the measured channel will take place as an attempt to evaluate the ability of COST 2100 to evaluate the performance of a system when a measured channel is available. The measure of performance will be the achievable sum rate capacity for all the microcells in the system.

The beamformer design for the CoMP Tx schemes described above, will follow two different approaches, namely, the zero forcing (ZF) and the signal to leakage and noise ratio (SLNR). The aim for the different beamformer design is to evaluate how the sum rate will be affected. For the JP technique the ZF and the SLNR beamforming will be used. The PJP and the CB will only use the SLNR beamforming design.

The structure of this thesis is as follows. This chapter provides information regarding the coordinating multi-point technology and what techniques are used in the downlink. In Chapter 2 the system models for the JP, PJP and the CB are presented. The ZF and SLNR beamformers are also described as well as how the beamforming weights are derived. In Chapter 3 the COST 2100 channel model is

presented and a brief description of some of its features are shown. In Chapter 4 measurement campaign is explained as well as how the channel was extracted from the measurements. The results from the experiments and a discussion on them is presented in Chapter 5. The concluding remarks are made in Chapter 6 and the future work is presented in Chapter 7.

In this work a 3 microcell system is assumed, where each BS has $N_T = 4$ transmit antennas. All the users in the system are assumed to have $N_R = 1$ receive antenna. The number of BSs is $M = 3$ and the total number of users in the system is K .

2.1 Coordinated beamforming

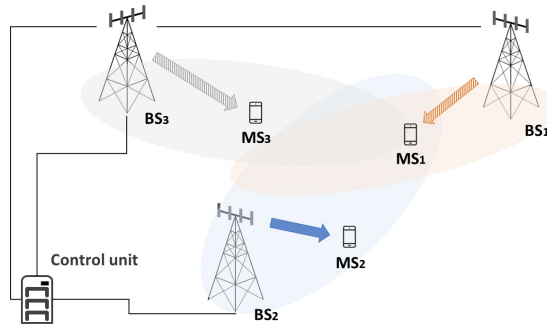


Figure 2.1: System representation of the coordinated beamforming scheme.

For the coordinated beamforming (CB) scheme it is assumed that only one BS is communicating with a specific user i at any time. The mathematical description of the CB system model is given by (2.1).

$$y_i = \mathbf{h}_i \mathbf{w}_i x_i + \sum_{k=1, (k \neq i)}^K \mathbf{h}_i \mathbf{w}_k x_k + n_i, \quad (2.1)$$

where \mathbf{h}_i is the $1 \times M \cdot N_T$ channel vector that is formed between the user i and all the BSs, \mathbf{w}_i is the $M \cdot N_T \times 1$ beamforming vector for user i . The entries of \mathbf{h}_i and \mathbf{w}_i are zeros except those entries that are corresponding to the serving BS. x_i is the data symbol for user i and n_i represents the identical independent distributed Gaussian noise with zero mean and variance σ^2 . The CB system layout is depicted in Figure 2.1.

The signal-to-interference-plus-noise ration (SINR) for user i is calculated as

$$SINR_i = \frac{\|\mathbf{h}_i \mathbf{w}_i\|^2}{\sigma^2 + \sum_{k=1, (k \neq i)}^K \|\mathbf{h}_i \mathbf{w}_k\|^2}, \quad (2.2)$$

The superscript $(\cdot)^H$ stands for the conjugate transpose and $\|\cdot\|^2$ is the Frobenius norm.

2.2 Joint Processing (JP)

A system that uses a JP CoMP transmission scheme utilizes all the BSs available to communicate with a user. The JP is shown in Figure 2.2. Using the JP improves the quality of the received signal at the receiver side but at the same time increases the overhead in the system, since the user data must be available to all BSs.

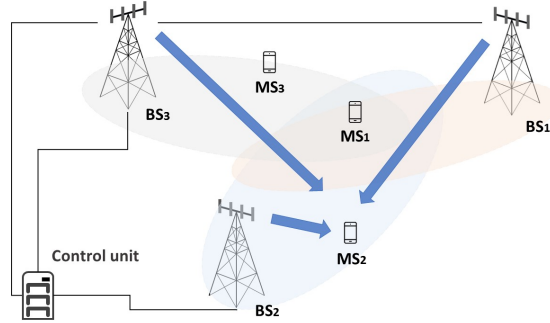


Figure 2.2: A JP scheme with 3 BSs communicate with MS 2.

For a specific user i the received signal y under the JP transmission scheme is given as

$$y_i = \mathbf{h}_i \mathbf{w}_i x_i + \sum_{k=1, k \neq i}^K \mathbf{h}_i \mathbf{w}_k x_k + n_i, \quad (2.3)$$

where \mathbf{h}_i is the $1 \times M \cdot N_T$ channel vector that is formed between the user i and all the BSs, \mathbf{w}_i is the $M \cdot N_T \times 1$ beamforming vector for user i and x_i is the data symbol for user i . The second term in (2.3) represents the multi-user interference. The SINR based on the received signal at user i is given as

$$SINR_i = \frac{\|\mathbf{h}_i \mathbf{w}_i\|^2}{\sigma^2 + \sum_{k=1, k \neq i}^K \|\mathbf{h}_i \mathbf{w}_k\|^2} \quad (2.4)$$

2.3 Partial Joint Processing (PJP)

As explained earlier, in a PJP scheme a user receives data only from BSs that belong in its active set and it is essentially a special case of JP. Thus, the amount

of (backhaul) data to be transmitted between the user and the BSs is reduced. The PJP is illustrated in Figure 2.3.

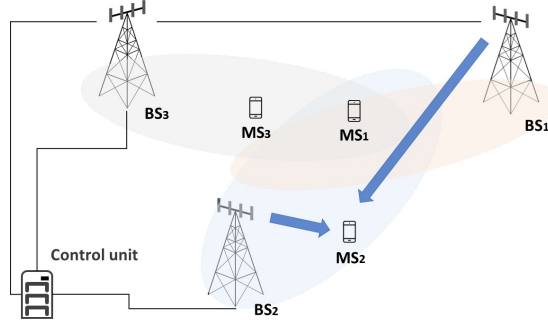


Figure 2.3: A PJP scheme with MS_2 having 2 BSs in its active set.

The received signal y for user i is given as

$$y_i = \mathbf{h}_i \mathbf{w}_i x_i + \sum_{k=1, k \neq i}^K \mathbf{h}_i \mathbf{w}_k x_k + n_i, \quad (2.5)$$

where \mathbf{h}_i is the $1 \times M \cdot N_T$ channel vector that is formed between the user i and the BSs that belong to the active set of user i , \mathbf{w}_i is the $M \cdot N_T \times 1$ beamforming vector for user i and x_i is the data symbol for user i . The second term in (2.5) represents the multi-user interference. The channel vector h and beamforming vector w contain $M' \cdot N_T$ non-zero values, where M' represents the BSs that belong in the active set of the user i , otherwise their elements equal to 0. Regardless of the size of the active set, the norm of the beamforming vector w equals unity.

The SINR based on the received signal at user i is given as

$$SINR_i = \frac{\|\mathbf{h}_i \mathbf{w}_i\|^2}{\sigma^2 + \sum_{k=1, k \neq i}^K \|\mathbf{h}_i \mathbf{w}_k\|^2} \quad (2.6)$$

2.4 Sum rate capacity

The metric of evaluating the performance of all studied CoMP transmission schemes will be the sum rate capacity. The sum rate capacity is given by

$$C = \sum_{k=1}^K \log_2(1 + SINR_k), \quad (2.7)$$

where K is the total number of users as mentioned earlier.

2.5 Transmit beamforming vectors

In this section the beamforming vectors used on the transmitter (BS) side for all CoMP schemes are described. Two different beamformers were used at the BS side based on two different design criteria. A zero-forcing (ZF) beamformer that follows the maximization of the SINR criterion and a beamformer that opts to maximize the Signal to Leakage and Interference Ratio (SLNR) of a specific user. The SLNR beamformer design is explained in [21] and it is briefly discussed in this section. For more details the reader is encouraged to read the cited article. For the ZF beamformer the well known beamforming matrix containing the pseudo-inverse of the channel matrix will be used.

2.5.1 SLNR Beamformer

The SLNR is defined as the total received power at user i over the total power leaked from that user to the neighboring users in the vicinity, plus the noise power. It is referred to, as leaked power cause the user of interest does not receive all of the transmitted power coming from its serving BS but instead some portion of it is received by other users which consider it as interference. The leakage term is depicted in Figure 2.4.

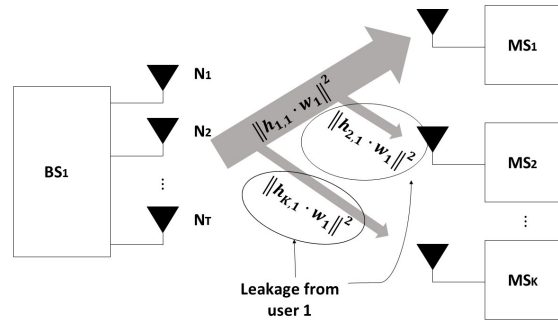


Figure 2.4: Illustration of the leakage term in a multi-user system.

As introduced in [21] and implemented in [22], by adopting the notation used in (2.2) the quantity that describes the leaked power from the i^{th} user to the rest of the users is given as

$$\sum_{k=1, k \neq i}^K \|\mathbf{h}_k \mathbf{w}_i\|^2 \quad (2.8)$$

The same requirement applies here as for the SINR case, the received signal power $\|\mathbf{h}_i \mathbf{w}_i\|^2$ of user i must be as large as possible while the total leaked power to the rest of the users $\sum_{k=1, k \neq i}^K \|\mathbf{h}_k \mathbf{w}_i\|^2$ must be kept to the minimum level.

CB

The SLNR for the CB transmission scheme, is given by the following formula

$$SLNR_i = \frac{\|\mathbf{h}_i \mathbf{w}_i\|^2}{\sigma^2 + \sum_{k=1, k \neq i}^K \|\mathbf{h}_k \mathbf{w}_i\|^2}, \quad (2.9)$$

where the channel vector \mathbf{h}_i has dimensions $1 \times N_T$, the transmit precoder vector \mathbf{w}_i is of size $N_T \times 1$.

JP and PJP

Since the PJP transmission scheme is a special case of the JP, the SLNR analysis for these schemes will be done together.

$$SLNR_i = \frac{\|\mathbf{h}_i \mathbf{w}_i\|^2}{\sigma^2 + \sum_{k=1, k \neq i}^K \|\mathbf{h}_k \mathbf{w}_i\|^2} \quad (2.10)$$

The matrices described in (2.9) and (2.10) have the same dimensions as the ones described in (2.4) and (2.6). The difference between (2.9) and (2.10) is the size of matrix \mathbf{h} and vector \mathbf{w} .

The design of the SLNR beamformer is based on the optimization problem described in [22] and aims to minimize the total interfering power that a user i is causing to the other users. In more detail, the goal is to select beamforming vectors \mathbf{w} so that (2.9) and (2.10) are maximized while \mathbf{w} is subjected to $\|\mathbf{w}\|^2 = 1$. The solution for this optimization problem is shown in [23] and is given by

$$\mathbf{w}_i^o \propto \max \text{eigenvector} \left(\left(\sigma_i^2 \mathbf{I} + \tilde{\mathbf{H}}^H \tilde{\mathbf{H}} \right)^{-1} \mathbf{h}_i^H \mathbf{h}_i \right), \quad (2.11)$$

where $\tilde{\mathbf{H}} = [\mathbf{h}_1^T \cdots \mathbf{h}_{i-1}^T \mathbf{h}_{i+1}^T \cdots \mathbf{h}_K^T]$ is an extended matrix that excludes \mathbf{h}_i only. The dimension of $\tilde{\mathbf{H}}$ is $(K-1) \times N_T$.

2.5.2 ZF Beamformer

The ZF beamformer design puts nulls in the directions other than the user of interest which results in minimizing the interference between neighboring users. Knowing the channel matrix \mathbf{H} of size $[N_R \times N_T]$ the beamforming matrix \mathbf{W} is given as the right pseudo-inverse of \mathbf{H}

$$\mathbf{W} = (\mathbf{H}\mathbf{H}^H)^{-1} \mathbf{H}^H, \quad (2.12)$$

where $(\cdot)^H$ and $(\cdot)^{-1}$ are the Hermitian transpose, and inverse operators respectively. The beamforming vector for user i is taken from column i of the beamforming matrix \mathbf{W} .

Channel Matrix Generation and the COST 2100 model

The model used for generating the channel realizations is based on the COST 2100 Geometric-based Stochastic Channel Model (GSCM). In GSCMs modeling, the distribution of the interaction objects or scatterers stochastically and based on the location of the interacting objects, the positions of the Tx and the Rx, the directional and delay properties of the different multipath components are calculated. When referring to the double-direction domains the Direction of Departure (DoD) and Direction of Arrival (DoA) are implied. The radio channel in COST 2100, and all other GSCMs, is a result of the superposition of different multipath components (MPCs) created from different propagation paths. The MPCs can either be single-bounce or double-bounce propagation components.

The COST 2100 channel model can be used for simulating the radio channel between a multiple antenna BS and single or multiple MS. The modeling process is specified once for the entire environment [1] by:

- Defining the location of clusters based on a stochastic model throughout the simulation environment
- Defining the so-called visible clusters regions
- Synthesizing the channel matrices based on the active clusters

The MPCs are mapped to the corresponding scatterers and are characterized by their delay, azimuth of departure (AoD), elevation of departure (EoD), azimuth of arrival (AoA) and elevation of arrival (EoA). Clusters are represented by MPCs with similar delays, azimuth and elevation.

There are three different types of clusters defined in the COST 2100 model as presented in Figure 3.1. Local clusters are comprised from single-bounce scatterers that are located around the MS and BS. Far clusters are divided into single-bounce and multiple-bounce clusters and are distributed throughout the simulation area. The local clusters are always visible from the BS or the MS but that is not necessarily true for the far-clusters where their visibility is determined by the visibility region. The visibility region defines the amount of active scatterers within a cluster for a limited geographical area. The last cluster type is called twin cluster and describes a multiple-bounce cluster with two identical representations as seen from the BS and the MS.

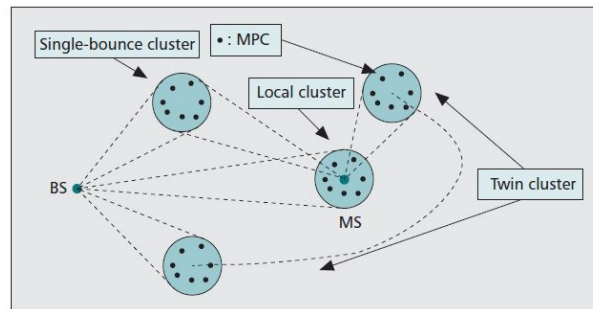


Figure 3.1: COST 2100 channel structure [1].

3.1 Visibility Region (VR)

The visibility region (VR) is a circular region with a fixed size inside the simulation area and determines the visibility of only one cluster. The VR gain which spans from 0 to 1 determines how visible is the cluster from the MS side. When multiple VRs overlap, multiple clusters are visible from the MS. Figure 3.2 illustrates the cluster visibility using the VR terminology.

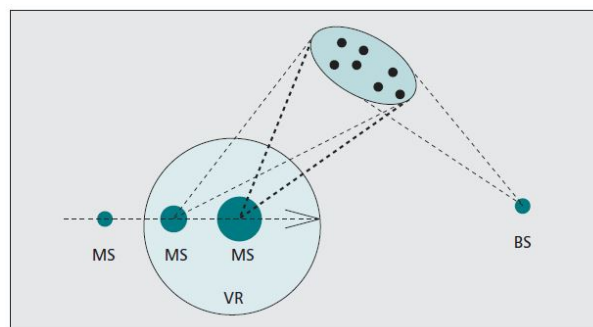


Figure 3.2: Illustration of the VR under the COST 2100 channel model [1].

3.2 COST 2100 features

3.2.1 Line of Sight

The Line of Sight (LOS) in COST 2100 is considered as a special case cluster with only one MPC, with a randomly scaled power with respect to the active cluster power. The visibility of the LOS component also depends on the VR which has its own size and distribution.

3.2.2 Polarization

The polarization behavior in COST 2100 is described on cluster level, meaning, that each MPC can contain four polarization components: vertical-to-vertical (VV) polarization, horizontal-to-horizontal (HH) polarization, vertical-to-horizontal (VH) and horizontal-to-vertical (HV). These polarization components can be projected onto the MIMO antenna array to form multipolarized subchannels.

The reader is encouraged to study referenced article [1] for more details regarding the COST 2100 model.

3.3 COST 2100 Implementation

The implementation of the COST 2100 model is given by a full description of the environment and the synthesis of the MIMO channel matrix by combining the double-direction channel with transmit and receive antenna steering vectors s_t and s_r :

$$\mathbf{H}(t, \tau) = \frac{1}{L} \sum_{n \in \mathcal{C}} V_n \sqrt{\frac{S_n}{L_n}} \left[\sum_{p=1}^P \alpha_{n,p} s_t(\Omega_{n,p}) s_r(\Psi_{n,p}) \delta(\tau - \tau_n^{(l)} - \tau_{n,p}^{(M)}) \right], \quad (3.1)$$

where L is the overall pathloss, which provides the dependence toward the BS-MS distance, \mathcal{C} is the set of visible clusters determined by the MS location, $\tau_n^{(l)}$ is the cluster-link delay, V_n are the cluster visibility gain accounting for the transmission in/out of the VR, S_n is the cluster shadow fading, L_n is the cluster attenuation which grows exponentially with the cluster excess delay, $\alpha_{n,p}$ is the complex Gaussian fading of the p^{th} MPC in cluster n , $\tau_{n,p}^{(M)}$ is the geometric delay, corresponding to the BS-to-scatterer-to-MS path, $\Omega_{n,p}$ and $\Psi_{n,p}$ are the DoD and DoA of the p^{th} MPC in cluster n and $\delta(\cdot)$ is the Dirac function.

Implementing equation 3.1 will derive the theoretical channel matrix in order to evaluate the CoMP schemes mentioned in previous sections. More specifically an adaptation of the COST 2100 model in a rural microcell environment as presented in [24] will be used. The frequency of operation of the system will be 2.6 GHz and the generated matrix will be used to compare the performance of the different CoMP transmission techniques with respect to the channel matrix acquired by the measurement campaign.

Propagation Measurements

The measurement campaign was carried out with the RUSK LUND channel sounder [25] at 2.6 GHz and a measurement bandwidth of 40 MHz. The measurements took place at the campus of the faculty of Engineering, LTH, Lund University, Lund, Sweden. The measurement environment can be best characterized as a suburban microcell environment. The chosen setup consists of three transmit BSs, each of which is equipped with a uniform antenna array with four vertically polarized antenna element having a half wavelength enter-element spacing as show in Fig.4.1.



Figure 4.1: The RUSK LUND channel sounder used in the measurement campaign.

The sounding signal is conveyed to each of the remote BSs locations through the optical backbone network of the campus by means of radio-over-fiber (RoF) transceivers. After being amplified to power of 30 dBm, the signal is broadcasted from each BS antenna element. The signal broadcasted by the BSs is received by an MS equipped with 64 dual-polarized antenna elements in a stacked uniform cylindrical array configuration. The 1536 (12 BS antenna elements \times 128 MS antenna elements) transmit-receive channels are sounded in a time-multiplexed fashion, all of the receive antenna elements being visited in succession prior to

switching to the next transmit antenna element. The data resulting from this operation is referred to as a snapshot. Please refer to [26] for more details about the equipment used. The transmit antennas were placed outside the windows at the second and third floors of four different buildings, which corresponds to 5 to 12 m above the ground level (10 to 20 m below the rooftop of surrounding buildings). The area in the middle of the selected buildings is an open area with a small lake surrounded by high leafy trees, as shown in Fig.4.2. The measurements took place in a predefined route circulating the lake, with a total length of about 490 m, at a very low walking speed (<0.5 m/s).

The propagation conditions between the MS and each of the BSs transmit antennas can be described as obstructed line-of-sight (OLOS), or non-line-of-sight (NLOS) due to the large leafy trees in the measurement area, as shown in Fig.4.2 and Fig.4.3. It should be noted that the intensity of the tree blockage varies from one MS position to another. Line-of-sight (LOS) condition between the MS and one of the BS occurs mainly when the MS is very close to one of the BSs. When the MS is far from the BSs, there were still possibilities of getting the optical LOS cleared between the MS and the different BSs. However, by detailed inspection, it was found that the first Fresnel zone at these locations was not clear.

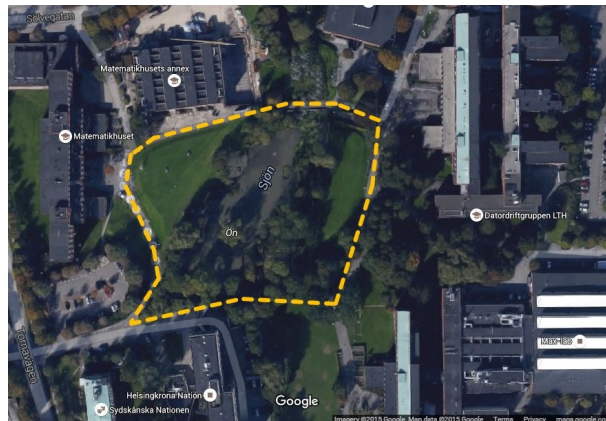


Figure 4.2: The path under which the measurement campaign took place. The simulated users were placed along this trail.

As mentioned earlier, the MS is provided with 128 antenna elements. In this work, we assume the MSs to have a single antenna. Therefore, the data of only four MS elements whose joint radio pattern is approximately isotropic on the azimuth plane is considered. In the first place, a power correction is applied to each of the remote transmit antenna elements in order to compensate for differences in gain due to antenna arrays, amplifiers, optical transceivers and fibers. The compensation method is based on the observation that the mean path loss over a large area for co-located transmit antenna elements must be identical. Then, the transmit-receive channels of these four elements are non-coherently combined, which result in having a channel vector of 12 entries for each snapshot (12 BS antenna elements \times 1 MS antenna element). The total number of measured snapshots is 4200, where

the MS was wheel-triggered each a wavelength.

Consequently, the size of the channel matrix for each user is a vector of 12 elements, corresponding to the total number of BS antenna elements. When a user is not served by all 3 BSs then the respective entries in the channel vector are zero and only the serving BS is represented by non-zero entries. The total number of measured snapshots is 4200 and, in this work, it is assumed that each snapshot can represent an individual user. The justification for this assumption comes from the fact that the measured channel is considered static.



Figure 4.3: Photo of a part of the measurement route showing the MS unit.

Chapter **5**
Results

The location of each user can be tracked on a specific path on which the measurements, presented in [20], took place. Two successive locations are separated by a wavelength distance. The possible locations that a user could have during the simulation follows the same principle described for the measured channel. In this work the distribution of the users is examined and its effects on the system performance are presented.

It is considered that the all the BSs have the same transmitted power. The beamformer design for both the SLNR and ZF techniques considers equal power allocation to all users with $\|w\|^2 = 1$.

The channel matrix used for both methods mentioned above represents a frequency selective channel with LOS and OLOS components.

5.1 Performance evaluation under measured channel matrices

Three CoMP transmission schemes were compared under a microcell suburban channel environment, namely the Joint Processing (JP), the Partial Joint Processing (PJP) and the Coordinated Beamforming (CB) techniques. The comparison was done using the sum-rate capacity metric while two different approaches were considered. The first method considers the channel matrix coming from measurements acquired in [20] while the second considers the channel matrix generated using the COST 2100 channel model. Adaptations to the stochastic parameters of COST 2100 were made in order to match the measurement environment and make the comparison between the two methods more valid. The JP scheme was studied under two different beamforming techniques, the SLNR and the ZF. The PJP and CB schemes were studied under the SLNR beamformer only. In all cases full cooperation between the BSs in the system and full channel state information is assumed.

Figure 5.1 depicts the sum-rate capacity for the two CoMP transmission schemes when the channel matrix is generated using the measurements from [20]. It is clear that the PJP transmission scheme outperforms the CB scheme by far. That was to expected since using the PJP transmission scheme implies that more than one BS can communicate with a user at a given time. On the contrary, the JP with SLNR transmission scheme does not seem to comply to that same logic and the ergodic capacity of the system is lower compared to when the PJP scheme was

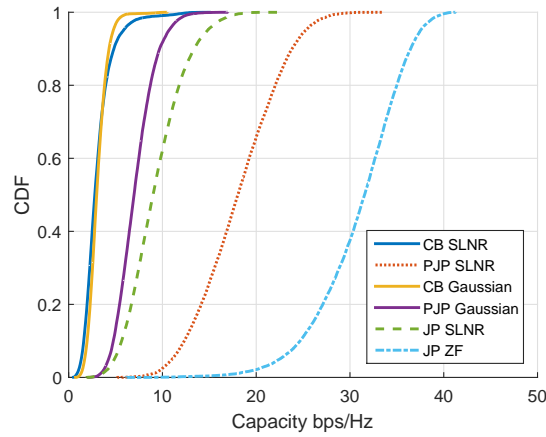
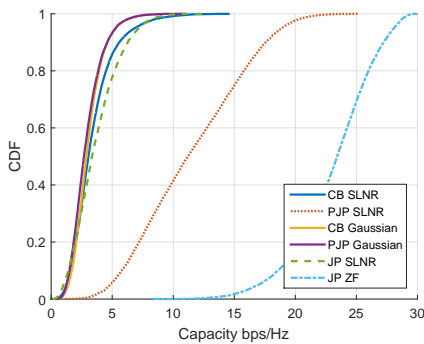
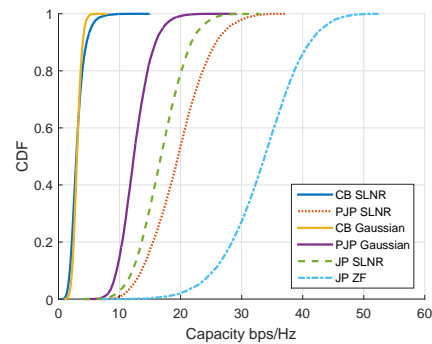


Figure 5.1: Sum rate capacity for 6 randomly distributed users when $\text{SNR} = 15\text{dB}$ is considered. The results are based on the channel matrix generated by the measurement data.

used. A possible explanation for this disparity might be the increase of interference when more BSs are involved to the transmission. Finally, one can observe that the performance of the CB transmission scheme under the measured channel, follows closely the results of the Gaussian channel. It seems that the CB transmission scheme cannot take advantage of the non-white (received signal power is dependent of the BS-MS distance) channel described by the measurements thus result in the same performance as a white Gaussian channel.



(a) 4 users randomly distributed.



(b) 8 users randomly distributed.

Figure 5.2: Sum rate capacity for 4 and 8 randomly distributed users when $\text{SNR} = 15\text{dB}$ is considered. The results are based on the channel matrix generated by the measurement data.

In Figure 5.2 the system performance for SNR equal to 15dB when 4 and 8 users are present, is shown. Irrespective of the number of users it is visible that

despite the scaling of the results, the capacity curves follow the same trend, that is, the JP is under-performing compared to PJP. When 4 users are present in the system the JP transmission scheme is performing similarly to the CB scheme. On the other hand when 8 users are present in the system, the JP scheme is still under-performing compared to the PJP. A possible reason for that behavior is that the PJP scheme only uses the strongest links between the BSs and a specific user. The useful links are decided based on a threshold between the BSs links and the strongest link off all the available links. That way the SNR remains high and the effect of the interference low. Under the JP scheme, all the BSs are communicating with the user of interest irrespective of the link strength which introduces interference while at the same time the received signal strength remains low.

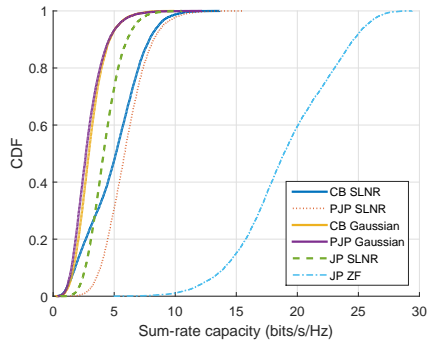
5.1.1 Effect of user spacing

So far the users in the system were distributed randomly on the path shown in Figure 4.2. In this section the effect of the users’ distribution on the system’s performance is examined. An interesting approach would be to distribute the users uniformly on the measurement path with a varying spacing between them and examine how effectively the system can serve the present users with respect to inter-user distance. Although one can argue that the distribution of users would be more realistic if done under an area instead of a straight line, the motivation behind this choice is to compare the simulated channel with the measured one, in a fair matter.

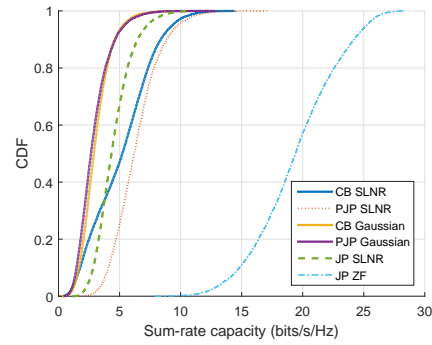
In Figure 5.3 the performance of the system for different number of uniformly distributed users is shown. The effect on the system performance for a distance spacing of 5 and 10m is also presented.

The first thing one can notice is that the CB transmission scheme performs very close to the JP and PJP schemes and in the case of 4 users it even outperforms the JP. From these results, using the measurement data to generate the channel, it is evident that increasing the distance between the users will increase the performance of the system for the JP and PJP transmission schemes slightly. The PJP transmission scheme when 6 users are present in the system, achieves almost the same sum-rate capacity as when 8 users are present. At the same time the JP outperforms the PJP transmission scheme which might be caused by the increase in the number of users and performance restrictions of the PJP due to its BS selection threshold. A decrease PJP’s threshold should lead to the PJP performing closer to the JP as the PJP represents a special case of JP.

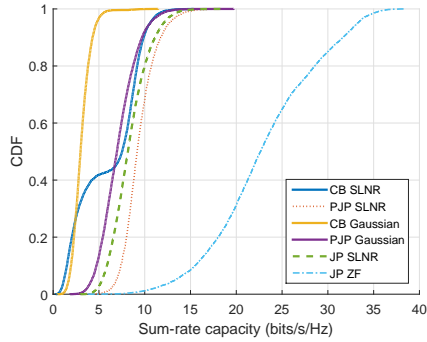
The shape of the CB capacity curve when 6 and 8 users are present in the system reveals that along the movement path of the users the channel conditions were more favorable to the users for some locations, a fact associated with the LOS components or constructive MPCs reaching the receiving antenna on the user side.



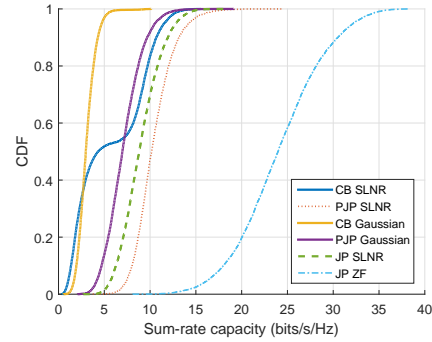
(a) 4 users with 5m spacing.



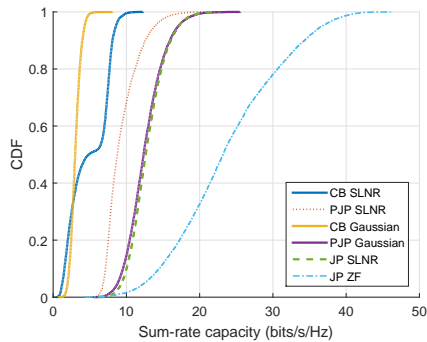
(b) 4 users with 10m spacing.



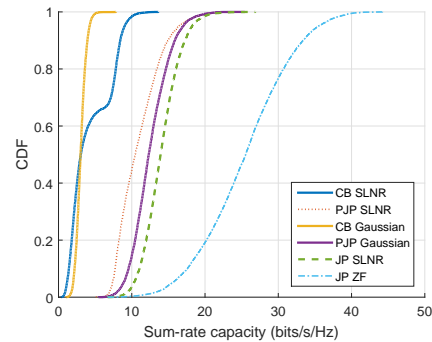
(c) 6 users with 5m spacing.



(d) 6 users with 10m spacing.



(e) 8 users with 5m spacing.



(f) 8 users with 10m spacing.

Figure 5.3: Sum rate capacity for different number of uniformly distributed users with 5m spacing on the left and 10m spacing on the right. The channel matrix was generated from the measurement data.

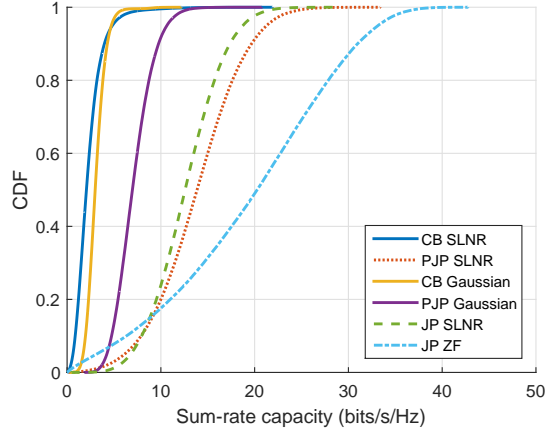


Figure 5.4: Sum rate capacity for 6 randomly distributed users when $\text{SNR} = 15\text{dB}$ is considered. The channel matrix was generated using the COST 2100 model.

5.2 Performance evaluation based on generated channel matrices using COST 2100

The performance of the two CoMP schemes when the channel matrix generated by the COST 2100 is presented in Figure 5.4. The calculated capacities are compared against a Gaussian channel to provide an insight of the achieved performance.

The performance of the CB transmission scheme, when the COST 2100 generated channel was used, is lower compared to the Gaussian channel, a reasonable fact as the COST 2100 represents a more realistic channel environment representation than its theoretical counterpart. At the same time the PJP transmission scheme provides higher sum rate capacity when the simulated channel is used compared to the Gaussian. Moreover, it yields better results compared to both the CB and the JP transmission schemes. A comparison between JP and PJP underlines that PJP performs better which might be a result based on the assumption mentioned before.

In Figure 5.5 the system performance for 4 and 8 users is presented. As expected the sum-rate capacity is directly related to the number of users, which explains the decrease in performance when 4 users are present compared to 6 and the increase when 8 users are present. An important note to make regarding the system’s performance under the presence of 8 users is that the JP with SLNR yields almost the same ergodic capacity compared to the JP with ZF. The PJP transmission scheme yields higher ergodic capacity compared to the JP with SLNR for 6 and 4 users and performs better at 10th and 90th percentile. At the same time the PJP scheme provides higher outage capacity (10th percentile) than the JP with ZF in the case of 6 and 8 users but produces lower ergodic capacity.

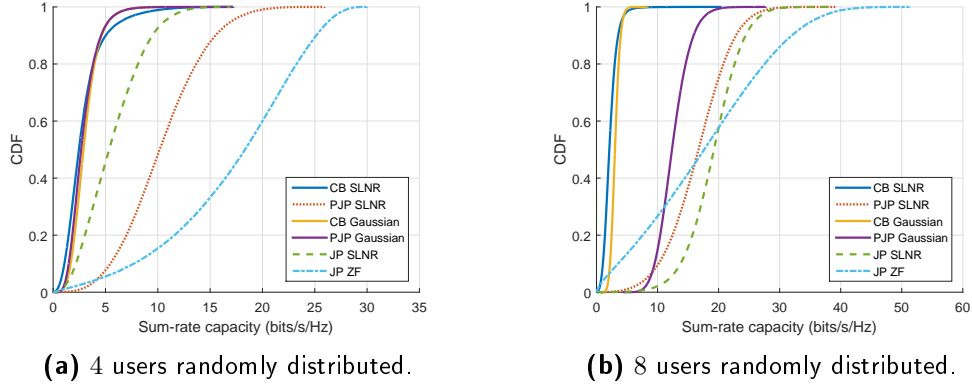


Figure 5.5: Sum rate capacity for 4 and 8 randomly distributed users for $\text{SNR} = 15\text{dB}$. The channel matrix was generated using the COST 2100 model.

5.2.1 Effect of user spacing

As explained in the previous section, it would be insightful to evaluate the performance of the system when the users are uniformly distributed in a specific area. In this section the effect on the sum rate capacity of two different inter-user spacings will be presented as well as justification on the results.

Observing Figure 5.6 it is easy to notice that the JP transmission scheme performs better than the CB and PJP when 6 and 8 users are present in the system. For 8 users it is noticeable that the ZF beamformer starts to under perform. A similar behavior can be seen in the JP ZF capacity curves for 6 users where the curves are starting to become straight lines.

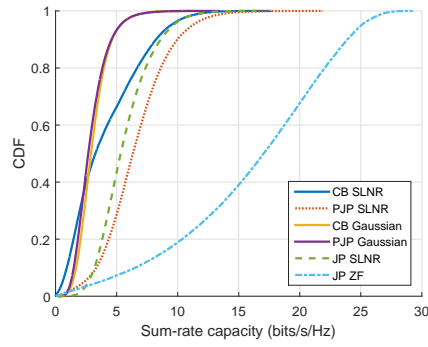
When comparing the PJP and JP with SLNR it is clear that the increase in the number of users will result in the JP to have better performance than the PJP. This seems reasonable as all the BSs are involved in the transmission process. It is expected that if the selection threshold is decreased that the PJP and JP would provide similar results as the PJP comprises a special case of JP.

Comparing the COST 2100 generated channel with the Gaussian, provides some interesting results. Using the PJP transmission scheme one can notice that for 8 users, using the Gaussian channel yields higher ergodic capacity than when using the COST 2100 channel. This seems reasonable as the COST 2100 channel model provides a more realistic channel description.

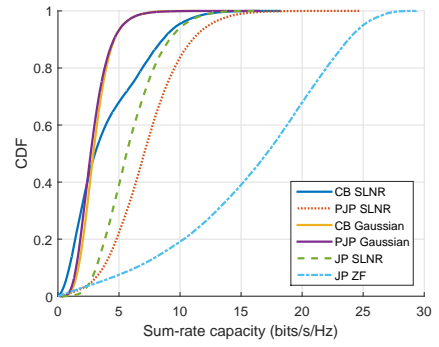
5.3 Performance Comparison between measured channel and COST 2100 channel

5.3.1 Randomly distributed users

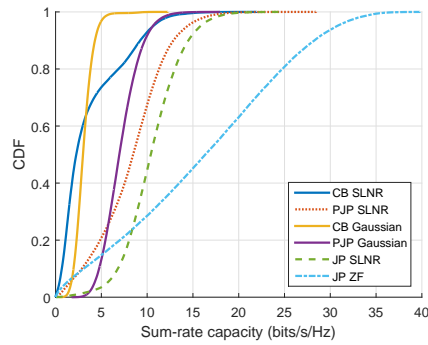
Figure 5.7 shows the performance difference of the CoMP transmission techniques between the COST 2100 and measured channels while Table 5.1 summarizes the



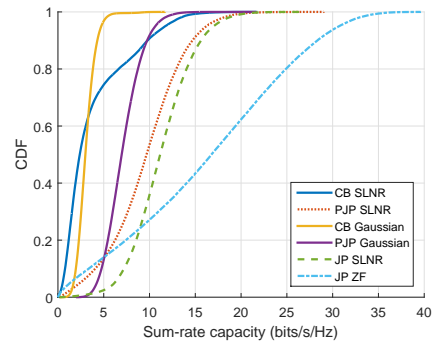
(a) 4 users with 5m spacing



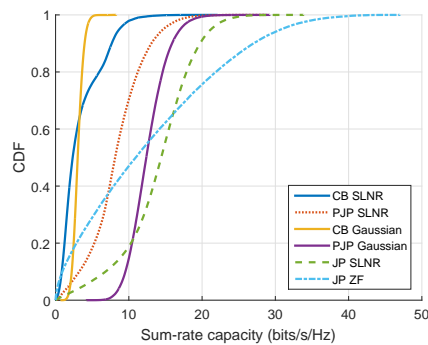
(b) 4 users with 10m spacing



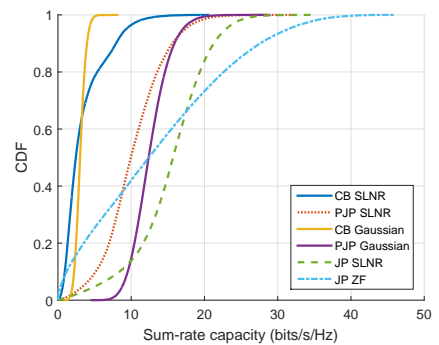
(c) 6 users with 5m spacing



(d) 6 users with 10m spacing



(e) 8 users with 5m spacing



(f) 8 users with 10m spacing

Figure 5.6: Sum rate capacity for different number of uniformly distributed users with 5m spacing on the left column and 10m spacing on the right column. The channel matrix was generated using the COST 2100 model.

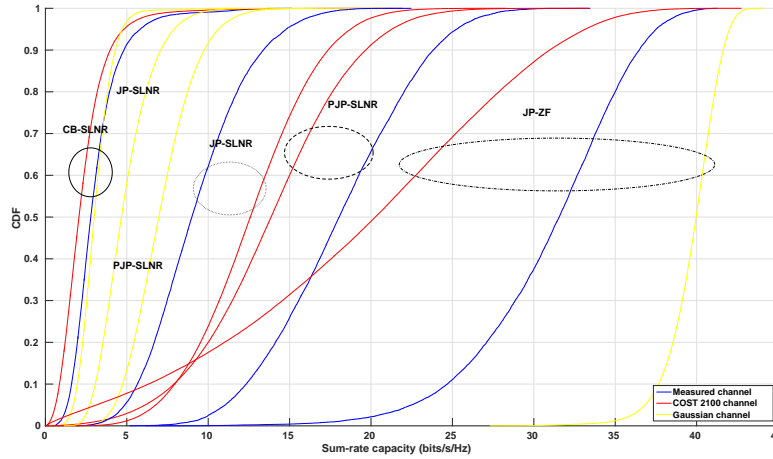


Figure 5.7: Comparison of CoMP techniques between the COST 2100 and measured channel. These results assume 6 randomly distributed users and $\text{SNR} = 15\text{dB}$.

performance of CoMP transmission techniques from Figures 5.1, 5.2, 5.4 and 5.5. It is clear from Figure 5.7 that the COST 2100 underestimates the performance of system for the CB, PJP and JP with ZF while overestimating the performance when the JP with SLNR is considered. From the values in Table 5.1 one can notice that when the COST 2100 is considered the JP with SLNR and the PJP perform closely. That is clearly not the case when the measured channel is considered for the calculations. The CB transmission scheme performs almost the same regardless of the way the channel matrix was generated. A closer look at the results of Table 5.1 reveals that the same situation occurs regardless of the number of users. It is evident that the COST 2100 model can estimate the relative performance for different transmission schemes for distributed MIMO systems although differences between the measurements and the theoretical model still exist. In following sections an attempt to investigate the reason behind this performance discrepancy will be made.

5.3.2 Uniformly distributed users

Figure 5.8 depicts the performance comparison between the COST 2100 generated channel and the measured channel for 6 uniformly distributed users with 10m spacing between them.

The first thing to notice is that the JP with ZF and the CB perform better under the measured channel a fact that was true for the random user distribution as well. The JP with SLNR performs better under the COST 2100 channel probably due to the cluster positions. The cluster positions for the COST 2100 channel will be studied in a following section with the hope to provide a clearer insight on the performance disparity. The CB scheme provides similar performance for the

SNR =15dB		COST 2100			Measured channel		
		Number of users			Number of users		
		4	6	8	4	6	8
10th percentile (bps/Hz)	CB	1.07	0.86	1	1.58	1.61	1.85
	PJP	5.47	7.90	10.16	5.77	12.33	13.6
	JP SLNR	2.17	7.95	13.75	1.40	5.65	12.11
	JP ZF	7.71	6.33	3.52	18.57	24.69	25.39
50th percentile (bps/Hz)	CB	2.46	2.06	2.1	3.16	2.78	2.92
	PJP	10.18	13.86	16.71	11.21	18.05	19.58
	JP SLNR	5.35	12.59	19.24	3.35	8.99	16.77
	JP ZF	18.34	20.27	17.63	23.43	31.56	33.81
90th percentile (bps/Hz)	CB	5.03	3.97	3.54	5.59	4.83	4.61
	PJP	15.51	19.67	22.84	17.55	23.82	25.86
	JP SLNR	9.49	17.36	24.43	6.28	13.39	21.77
	JP ZF	25.14	30.97	31.98	27.24	36.48	41.21

Table 5.1: Concentrated results for the sum-rate capacity performance between the COST 2100 generated channel and the measured one. The results presented in the table assume SNR =15dB and random user distribution.

COST 2100 channel regardless of the number of users and the inter-user spacing as can be seen from the Table 5.2. For the rest of the schemes, increasing the inter-user distance leads in an increase in performance.

Comparing the results under different channel matrices and inter-user distance of 10m provides the same conclusion as in the random distribution of users. The COST 2100 model underestimates the performance of the CB, PJP and JP with ZF schemes and overestimates the performance of the JP with SLNR scheme compared to results calculated from the measured channel. For an inter-user spacing of 5 and 20m the COST 2100 model estimates the performance of the PJP transmission scheme fairly accurate compared to the measured channel with the highest percentage difference being 12.82%, occurring when 4 users with 10m spacing were consider. Another interesting thing to comment is that the JP with ZF provides lower performance regardless of the inter-user spacing when compared to the results coming from the measured channel. As mentioned earlier a more detailed investigation on the COST 2100 parameters is needed in order to be able to explain performance difference.

5.4 System performance variation based on inter-user distance

In the previous sections the sum-rate capacity of the system was analyzed for different inter-user distances for both a measured channel matrix and a channel

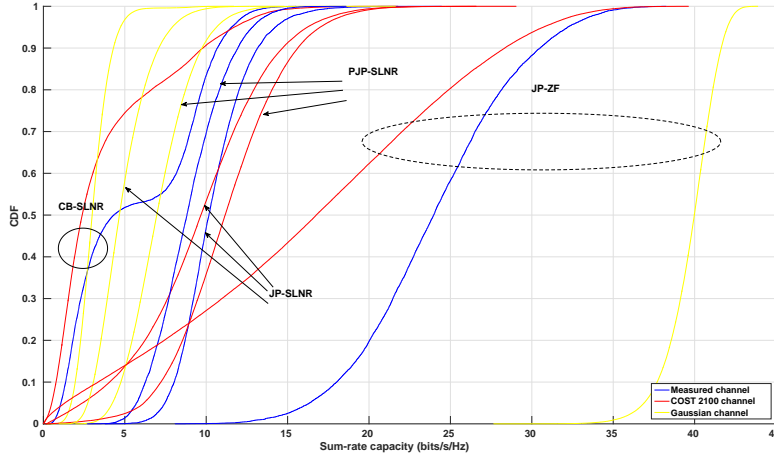


Figure 5.8: Performance comparison of CoMP transmission schemes under the COST 2100 and measured channels. The graphs shown here correspond to 6 users with 10m separation and SNR =15dB.

matrix generated by the COST 2100 model. In this section the performance variation of the system based on the inter-user distance is presented as shown in Figure 5.9.

The performance evaluation was done using the 5m inter-user as the base case and comparing it against an 10 and 20m inter-user distance. The left column represents the evaluation done under the COST 2100 generated channel matrix while the right one represents the evaluation under the measured channel.

Analyzing the performance under the COST 2100 generated channel, one can notice that the PJP transmission scheme is the most affected by the inter-user spacing and in some cases the sum-rate capacity can increase more than 50%. In general, one can conclude that as the inter-user distance becomes larger the sum-rate capacity of the system increases. A possible reason as to why the PJP scheme is the most affected might be the selection threshold that the PJP is using in order to decide on the active set of each user. If the inter-user distance is getting larger the channel links for a user might improve thus the size of the active set will become larger and more BSs will communicate with that specific user.

The JP transmission scheme with SLNR is the second most affect transmission scheme when the inter-user distance is increased and for 8 users present the sum-rate capacity can increase almost 25% percent. The same trend seems to apply here as in the PJP transmission scheme, that is, an increase in the inter-user distance will increase the sum-rate capacity of the system. It is possible that by increasing the inter-user distance the links between the users become more uncorrelated, a fact that leads to increased sum-rate capacity.

The JP with ZF transmission scheme is almost unaffected by the change in

		COST 2100			Measured channel		
		Number of users			Number of users		
		4	6	8	4	6	8
5m	CB	3.25	2.26	2.33	5.14	7.53	4.86
	PJP	6.33	8.47	8.13	5.85	9.17	8.75
	JP SLNR	5.33	10.4	14.41	4.13	8.17	12.63
	JP ZF	17.04	16.34	10.93	18.89	22.65	23.19
10m	CB	3.03	2.38	2.44	5.23	4.33	3.04
	PJP	7.10	9.67	9.95	6.19	10.17	10.47
	JP SLNR	5.61	11.16	15.71	4.34	8.82	13.93
	JP ZF	17.09	16.75	12.41	19.41	23.97	25.55
20m	CB	3.11	2.57	2.39	3.97	3	2.95
	PJP	8.04	11.53	13.17	7.12	12.23	13.47
	JP SLNR	5.89	12.11	17.03	4.41	9.76	15.76
	JP ZF	17.07	16.98	13.02	21	26.25	28.39

Table 5.2: CoMP transmission schemes sum-rate performance for uniformly distributed users in the simulation area for SNR =15dB. The results consider the 50th percentile of the capacity curve.

the inter-user distance and the same is also true for the CB transmission scheme. The CB and JP with ZF transmission schemes are the only schemes that are affected negatively when the inter-user distance changes, a fact probably caused from limitations of the SLNR related to the inter-user distance.

Considering the measured channel, the trend is similar as in the COST 2100 channel. The transmission schemes yield higher sum-rate capacity when the inter-user distance is increased. Once again, the PJP scheme is the one that is affected the most (positively) from the the increase in the inter-user distance compared to the rest of the schemes. The JP with ZF in the case of the measured channel provides a larger increase in sum-rate capacity for both inter-space distance compared to the COST 2100 generated channel. The CB scheme is the only transmission scheme that is affected negatively by increasing the inter-user spacing.

Overall, Figure 5.9 provides a more detailed view of how the system performance varies in terms of the inter-user distance. For both channel matrices (COST 2100 and measured) the schemes that are more dependent to the inter-user distance are the PJP followed by the JP with SLNR.

5.5 Changing the COST 2100 model parameters

In this section, an attempt to investigate some of the basic parameters of the COST 2100 model will be made and how these changes will affect the system performance will be shown. Finally, a comparison against the measurement channel will be done in order to determine if the COST 2100 generated channel is describing the

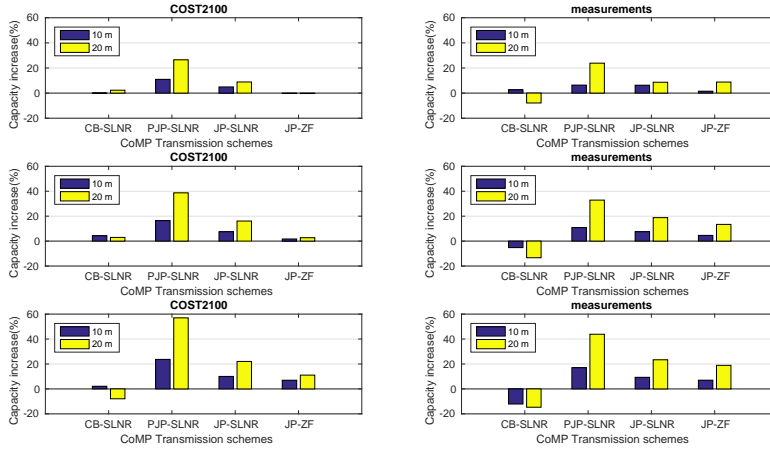


Figure 5.9: Sum-rate capacity variation with respect to inter-user distance change. The base case is 5m. The 3 rows correspond to 4,6 and 8 users in the system respectively.

measured channel effectively. Specific values for indoor and rural environments already exist and are validated from measurements. On the contrary, that is not the case for sub-urban microcell environments. Based on the findings of the previous studies regarding the appropriate values for the COST 2100 parameters and comparing them against the environment which the measurements took place, the values for the parameters were intuitively chosen as shown in Table 5.3. These are the initial values for COST 2100 parameters investigated in this section.

COST 2100 parameters	
VR size (m)	20
LOS transition region (m)	95
LOS cut-off distance (m)	60
LOS VR size (m)	100
VR distribution	Poisson

Table 5.3: Initial COST 2100 channel parameters. The simulations up until this point used these values.

5.5.1 LOS Visibility Region

As explained earlier the Visibility Region (VR) describes a geographical area inside which a cluster is visible from the user. Consequently, a LOS VR is a geographical area inside which the user has LOS of a BS. There are 3 variables related to the

LOS VR, the cut-off distance the VR size and the transition region LOS size . The cut-off distance defines an area around a BS outside of which the LOS component from that BS is non-existent, even if the user resides inside the LOS VR of that BS. The transition region defines a circular area around the center of the LOS VR and its size is smaller than the size of the LOS VR itself. The transition region also exists for the VRs connected to clusters and it is used to determine the visibility gain of the VR. The closer the user is to the center of the VR, the higher the visibility gain. If the user exceeds the transition region the visibility gain drops dramatically.

Since LOS is important to the channel link quality it will be interesting to see how the system performance will be affected when the size of the LOS VR is decreased. The simulation procedure was exactly the same as described in previous sections but this time the COST 2100 channel matrix was generated based on the changes in LOS VR size shown in Table 5.4.

COST 2100 parameter			
	Initial channel	Chan. ver. 2	Chan. ver. 3
LOS VR size (m)	100	50	150

Table 5.4: LOS VR size for different variations of the COST 2100 channel model.

The transition region for all the generated channels according to Table 5.4 was 95% of the LOS VR size. The cut-off distance was 60m in all cases. In Figure 5.10 the resulting performance for the PJP transmission scheme under the COST 2100 generated channels based on Table 5.4 is shown. The PJP was the transmission scheme of choice because it is affected more from the channel conditions due to the selection threshold it incorporates.

It is visible that by changing the size of the LOS VR, and hence how frequent is a LOS component present in the channel, the COST 2100 model cannot match the performance of the measured channel when the PJP transmission scheme is used.

In the next section the effect of the VR size of the clusters will be investigated in order to verify if the COST 2100 can model the measured channel with greater accuracy.

5.5.2 VR size

All the COST 2100 generated channels in this section will be compared against the COST 2100 channel presented in the beginning of this chapter and for which the results were presented. The base case for comparing will be the VR size to be equal 20m with a transition region of 5m. The comparison between the different COST 2100 channels is shown in Table 5.5.

In Figure 5.11 the results from the COST 2100 generated channel matrices based on the values of Table 5.5 are presented. The results in the graph are based on the PJP transmission scheme and SNR =15dB. It is clear that by changing the VR size did not provide similar statistics with the measured channel. The reason

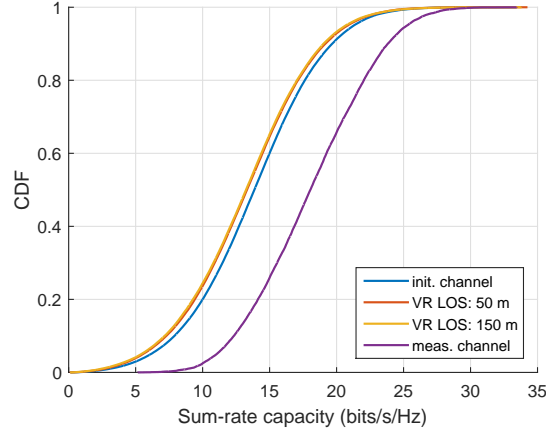


Figure 5.10: PJP performance for COST 2100 channels generated based on Table 5.4. The results assume 6 randomly distributed users and SNR = 15dB.

COST 2100 parameter			
	Initial channel	Chan. ver. 2	Chan. ver. 3
VR size (m)	20	35	50

Table 5.5: The values for the VR size of different generated COST 2100 channels.

for that is the way that the VR are created inside the simulation area. For the COST 2100 model the density of the VRs is given by (5.1).

$$\rho_C = \frac{N_c}{\pi (R_c - L_c)^2} [m^{-2}], \quad (5.1)$$

where R_c is the size of the VR and L_c the size of the transition area. N_c is the average number of far clusters. The product of the simulation area and the density of VRs gives the number of VR inside the simulation area. It is then straightforward that the greater the difference between the VR size and the transition region, the larger the number of VRs inside the simulation area.

The size of the VR did not seem to produce similar performance to the measured channel and it is probable that a more detailed study between the VR and transition region sizes is needed, in order to investigate if a statistical connection can be created between the COST 2100 generated channel and the measured one. In the following section the statistical distribution of the VRs locations will be investigated.

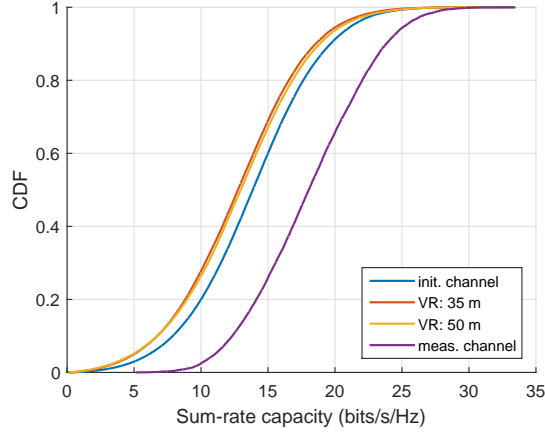


Figure 5.11: PJP performance for COST 2100 channels generated based on Table 5.5. The results assume 6 randomly distributed users and $\text{SNR} = 15\text{dB}$.

5.5.3 VRs location distribution

The COST 2100 assumes a Poisson distribution for the locations of the VRs. So far this setup did not seem to achieve similar performance with the measured channel. Hence, in this section 2 different distributions will be used for generating the locations of the VRs and the resulting sum-rate capacities will be used as means of evaluation against the measured channel sum-rate. The purpose is to identify whether or not the COST 2100 model can provide similar performance as the measured channel under a specific transmission scheme.

Hawkes process

The Hawkes process is a cluster process, which means that it is described by a center process and for each point of the center process, offsprings are generated based on a different process. The center process for Hawkes process is a Poisson process and the same goes for the process that generates the offsprings. The collection of the generated points forms the Hawkes process. In (5.2) the offspring intensity is shown for the Hawkes process.

$$\rho(x_1, x_2) = \frac{\alpha}{2\pi\sigma^2} e^{-\frac{1}{2\sigma^2}(x_1^2+x_2^2)}, (x_1, x_2) \in R^2 \quad (5.2)$$

Using the Hawkes process the locations of the VRs were generated. In Fig. 5.13b the VRs locations are shown together with the path of the all the possible user locations and the BSs locations.

Matérn process

For a Matérn process each point with a center c is uniformly distributed within a ball of radius r at c . The centers of the circles are not part of the point pattern.

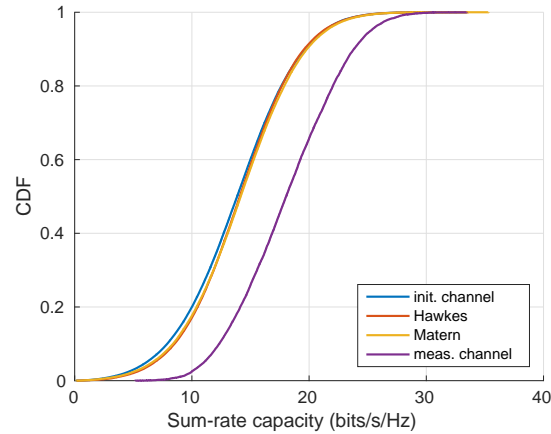
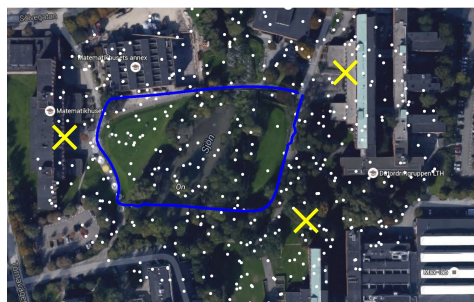


Figure 5.12: Sum-rate capacity of the PJP scheme for different distributions of the VRs. The results assume 6 randomly distributed users and $\text{SNR} = 15\text{dB}$.

For all the aforementioned VR distributions different channel matrices were generated using the COST 2100 model. Using these channel matrices the sum-rate capacity, for the CoMP transmission techniques mentioned earlier, was calculated. The results are presented in Fig. 5.12.

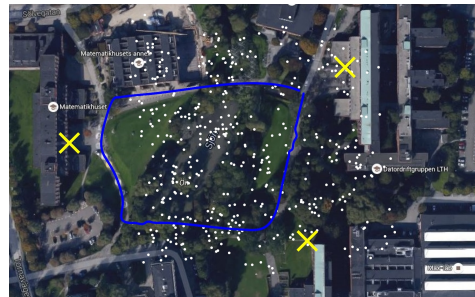
By looking at Fig. 5.12 one can conclude that Hawkes and Matérn distributions provide almost identical results compared to Poisson distribution. As mentioned earlier the comparison between different distributions of the VRs was made under a base case of the COST 2100 as shown in Table 5.3. Consequently, the reason for the similar results between the various VR distributions might be the size of the LOS VR. With a size of 150m for the LOS VR it is highly probable that the users in the simulation area will have a LOS to a BS, thus rendering the distribution of the VRs less significant. It might be possible, to match the performance of the measured channel if the parameters mentioned in this section are altered collectively instead of separately. Regardless, further investigation is required in order to be able to describe the measured channel statistically, using the COST 2100 channel model. In Fig. 5.13 the measurement environment is shown together with the VR locations for the processes mentioned above. As a reference the VR locations for the default distribution (Poisson) of the COST 2100 model is shown.



(a) Poisson distribution of the visibility regions



(b) Hawkes distribution of the visibility regions



(c) Matérn distribution of the visibility regions

Figure 5.13: Illustration of the VRs locations. The VRs are shown with white, the BSs locations are marked with yellow and the possible user locations with blue.

Conclusions

Several findings resulted from the investigation held in this thesis work. First the conclusions for the comparison of the CoMP transmission schemes will be presented followed by the findings related to the attempt to describe the measured channel using the COST 2100 channel model.

The Coordinated Beamforming (CB) performed the lowest compared to the rest of the CoMP transmission schemes irrespective of the number of users. Also, the number of users did not affect the ergodic sum-rate capacity to a significant amount, a not so surprising fact as under the CB, only one BS is serving a user.

The Partial Joint Processing (PJP) performs better than the CB and the Joint Processing (JP) with SLNR when 4 or 6 users are present but for 8 users it performs worse compared to the JP with SLNR. Although PJP performs less than JP with ZF when 4 or 6 users are present, for 8 users the performance disparity is much smaller. The PJP takes advantages of the selection threshold in order to create an active set for each user. Hence, only the BSs with the highest quality links communicate with a user, keeping the SINR level high. For the case of uniformly distributed users, the PJP transmission scheme under the COST 2100 channel performs worse than the JP with SLNR for all the inter-user spacings studied here (e.g. 5m, 10m, 20m) and for 6 and 8 users present.

The JP with SLNR outperforms the CB transmission scheme regardless of the number of users in the system, but worse than the JP with ZF. The reason for that is because ZF removes the effect of the interference completely, while the SLNR is a technique for mitigating interference. For the case of uniformly distributed users, the JP with SLNR performs better than JP with ZF when 8 users are present regardless of the inter-user spacing. On average, the JP with SLNR is performing similarly for various inter-user distances, so it is not the case that the JP with SLNR performs better when the number of users is increased, but rather, that the JP with ZF is under-performing. A possible explanation could be the distribution of the Visibility Regions (VRs).

Comparing the performance of the CoMP transmission schemes between the measured channel and the COST 2100 channel there are a few points to make. Initially, for a randomly distributed number of users the COST 2100 channel underestimates the ergodic sum-rate capacity for all CoMP transmission schemes except the JP with SLNR. For a number of uniformly distributed users, the COST 2100 channel again underestimates the ergodic sum-rate capacity of all CoMP schemes except the JP with SLNR. The PJP performance is close to the one estimated

from the measured channel and the same can be said for the CB transmission scheme. An important finding to mention is that the COST 2100 model is able to estimate the relevant performance of various distributed MIMO transmission schemes accurately when compared to channel measurements. At the same time there are indeed difference in the performance between the COST 2100 and measured channel which are probably caused by values that do not exactly match the measurement environment values, for the COST 2100 parameters. For the randomly distributed users, the performance deviation between the measured and COST channel for the CB transmission scheme was 34.95%, for the PJP 30.23%, for the JP with SLNR 28.59% and for the JP with ZF 55%.

It was found that the probability of a randomly distributed user being served by 1 BS was 0.77 for the measured channel, and 0.71 for the COST channel. At the same time, when a Gaussian channel was consider this probability dropped to 0.19 while the probability of that user being served from 2 BSs was increased (0.18 and 0.23 respectively for the previous two channels) to 0.44. The user was served by 3 BSs with a probability of 0.047 for the measured channel, 0.035 for the COST channel and 0.37 for the Gaussian channel. From these observations, we can deduct that the user position will affect the choice of the transmission technique.

Varying the values of basic COST 2100 parameters such as the size of the VRs, the size of the LOS VRs and the distribution of the VRs did not cause noticeable change to the results. The changes in the VR and LOS VR as shown from the capacity graphs did not affect the capacity estimation for the measured channel and the same behavior was observed for different distributions of the VRs in the simulation area.

The availability of measured channel data created a lot of opportunities for experimentation with the COST 2100 channel model. An in-depth investigation of its parameters can be studied for the purpose of the modeling a sub-urban microcell environment more accurately. A more detailed investigation might be able to reveal the reason for the performance estimation deviation between the COST 2100 and the measured channel as shown in this work. An important consideration should be the VR distribution and its connection to the LOS VRs size. Gaining more insight about the relationship of these two parameters will help to answer some of the assumptions stated in previous chapters. Finally a deeper look into the size of the VRs must be taken in order to be certain that the chose values are representative of the channel one wants to simulate.

References

- [1] L. Lingfeng et al. The COST 2100 MIMO channel model. *Wireless Communications, IEEE*, 19(6):92–99, December 2012.
- [2] 3GPP TR 36.814. Further advancements for E-UTRA physical layer aspects. Technical report, 3GPP, 03 2010.
- [3] M. Bengtsson et al. D1.4 initial report on advanced multiple antenna systems. Technical report, Wireless World Initiative New Radio WINNER+, 01 2009.
- [4] K. Okubo, Chang-Jun A., T. Omori, and K.-Y. Hashimoto. Enhancement of cell-edge throughput performance with CoMP transmission using QO-STBC scheme. In *Consumer Electronics (GCCE), 2013 IEEE 2nd Global Conference on*, pages 496–499, Oct 2013.
- [5] A. Papadogiannis, E. Hardouin, and D. Gesbert. A framework for decentralising multi-cell cooperative processing on the downlink. In *GLOBECOM Workshops, 2008 IEEE*, pages 1–5, Nov 2008.
- [6] I. Akyildiz, D. Gutierrez-Estevez, and E. Chavarria Reyes. The evolution to 4G cellular systems: LTE-advanced. *Physical Communication*, 3(4):217 – 244, 2010.
- [7] A. Papadogiannis, E. Hardouin, and D. Gesbert. Decentralising multicell cooperative processing: A novel robust framework. *EURASIP Journal on Wireless Communications and Networking*, 2009(1):890685, 2009.
- [8] A. Papadogiannis, H.J. Bang, D. Gesbert, and E. Hardouin. Downlink overhead reduction for multi-cell cooperative processing enabled wireless networks. In *Personal, Indoor and Mobile Radio Communications, 2008. PIMRC 2008. IEEE 19th International Symposium on*, pages 1–5, Sept 2008.
- [9] C. Wan and J.G. Andrews. Downlink performance and capacity of distributed antenna systems in a multicell environment. *Wireless Communications, IEEE Transactions on*, 6(1):69–73, Jan 2007.
- [10] M. Alatossava, A. Taparugssanagorn, V.-M. Holappa, and J. Ylitalo. Measurement based capacity of distributed MIMO antenna system in urban microcellular environment at 5.25 GHz. In *Vehicular Technology Conference, 2008. VTC Spring 2008. IEEE*, pages 430–434, May 2008.

- [11] Z. Xinsheng and Y. Xiaqing. Downlink ergodic capacity analysis for wireless networks with cooperative distributed antenna systems. In *Communications (ICC), 2012 IEEE International Conference on*, pages 5911–5915, June 2012.
- [12] L. Buon Kiong, M.A. Jensen, J. Medbo, and J. Furuskog. Single and multi-user cooperative MIMO in a measured urban macrocellular environment. *Antennas and Propagation, IEEE Transactions on*, 60(2):624–632, Feb 2012.
- [13] J. Liu, Y. Chang, Q. Pan, X. Zhang, and D. Yang. A novel transmission scheme and scheduling algorithm for CoMP-SU-MIMO in LTE-A system. In *Vehicular Technology Conference (VTC 2010-Spring), 2010 IEEE 71st*, pages 1–5, May 2010.
- [14] A.H. Muqaibel and A.N. Jadallah. Practical performance evaluation of coordinated multi-point (CoMP) networks. In *GCC Conference and Exhibition (GCCCE), 2015 IEEE 8th*, pages 1–6, Feb 2015.
- [15] X. Zhang, Y. Sun, X. Chen, S. Zhou, J. Wang, and N.-B. Shroff. Distributed power allocation for coordinated multipoint transmissions in distributed antenna systems. *Wireless Communications, IEEE Transactions on*, 12(5):2281–2291, May 2013.
- [16] J. Park, J. Kim, and W. Sung. Performance of distributed MISO systems using cooperative transmission with antenna selection. *Communications and Networks, Journal of*, 10(2):163–174, June 2008.
- [17] T.-R. Lakshmana. Dynamic coordinated multipoint transmission schemes, 2010.
- [18] Q. Li, Y. Yang, S. Fang, and G. Wu. Coordinated beamforming in downlink COMP transmission system. In *Communications and Networking in China (CHINACOM), 2010 5th International ICST Conference on*, pages 1–5, Aug 2010.
- [19] D. Zhangcheng, L. Xun, F. Shu, W. Gang, and Y. Chunlin. A novel coordinated beamforming scheme based on local feedback and quantization based combining in downlink comp system. In *Communication Technology and Application (ICCTA 2011), IET International Conference on*, pages 45–49, Oct 2011.
- [20] G. Dahman, J. Flordelis, and F. Tufvesson. On the cross-correlation properties of large-scale fading in distributed antenna systems. In *Wireless Communications and Networking Conference (WCNC), 2014 IEEE*, pages 160–165, April 2014.
- [21] A. Tarighat, M. Sadek, and A.H. Sayed. A multi user beamforming scheme for downlink MIMO channels based on maximizing signal-to-leakage ratios. In *Acoustics, Speech, and Signal Processing, 2005. Proceedings. (ICASSP '05). IEEE International Conference on*, volume 3, pages iii/1129–iii/1132 Vol. 3, March 2005.
- [22] M. Sadek, A. Tarighat, and A.H. Sayed. A leakage-based precoding scheme for downlink multi-user MIMO channels. *Wireless Communications, IEEE Transactions on*, 6(5):1711–1721, May 2007.

-
- [23] M. Sadek, A. Tarighat, and A.H. Sayed. Active antenna selection in multiuser MIMO communications. *Signal Processing, IEEE Transactions on*, 55(4):1498–1510, April 2007.
 - [24] M. Zhu, G. Eriksson, and F. Tufvesson. The COST 2100 channel model: Parameterization and validation based on outdoor MIMO measurements at 300 MHz. *Wireless Communications, IEEE Transactions on*, 12(2):888–897, February 2013.
 - [25] R. Thoma et al. Identification of time-variant directional mobile radio channels. *Instrumentation and Measurement, IEEE Transactions on*, 49(2):357–364, Apr. 2000.
 - [26] J. Flordelis, G. Dahman, and F. Tufvesson. Measurements of large-scale parameters of a distributed MIMO antenna system in a microcell environment at 2.6 GHz. In *Antennas and Propagation (EuCAP), 2013. 7th European Conference on*, pages 3026–3030, Gothenburg, Sweden, Apr. 2013.



LUND
UNIVERSITY

Series of Master's theses
Department of Electrical and Information Technology
LU/LTH-EIT 2016-501

<http://www.eit.lth.se>